

## COARSE RESOLUTION DEFECT LOCALIZATION ALGORITHM FOR AN AUTOMATED VISUAL PCB INSPECTION

ZUWAIKIE IBRAHIM<sup>1</sup>, SYED ABDUL RAHMAN AL-ATTAS<sup>2</sup> &  
ZULFAKAR ASPAR<sup>3</sup>

**Abstract.** One of the backbones in electronic manufacturing industry is the printed circuit board (PCB) manufacturing. Current practice in PCB manufacturing requires an etching process. This process is an irreversible process. Printing process, which is done before the etching process, caused most of the destructive defects found on the PCB. Once the laminate is etched, the defects, if exist would cause the PCB laminate to become useless. Due to the fatigue and speed requirement, manual inspection is ineffective to inspect every printed laminate. Therefore, manufacturers require an automated system to detect the defects online which may occur during the printing process. The defect is detected by utilizing wavelet-based image difference algorithm. Hence, this paper proposes an algorithm for an automated visual PCB inspection that is able to automatically locate and extract any defect on a PCB laminate. The algorithm works on the coarse resolution differenced image in order to locate the defective area on the fine resolution tested PCB image.

*Key words:* defect localization, coarse resolution, wavelets, PCB inspection

**Abstrak.** Satu daripada asas utama dalam industri pembuatan elektronik ialah pembuatan papan litar bercetak (PCB). Pembuatan PCB pada masa kini perlu melalui proses kikisan. Ini adalah proses satu hala. Proses cetakan yang dilakukan sebelum proses kikisan adalah penyebab utama kepada kecacatan pada PCB. Setelah PCB dikikis, kecacatan itu, jika ada menyebabkan PCB menjadi tidak berguna lagi. Disebabkan oleh keletihan dan keperluan kecekapan, pemeriksaan secara manual tidak efektif dilakukan untuk memeriksa setiap PCB. Oleh itu, pengilang memerlukan sebuah sistem automatik untuk mengesan kecacatan secara masa nyata yang mungkin berlaku semasa proses percetakan. Kecacatan itu akan dikesan dengan menggunakan algoritma pembezaan imej berasaskan wavelet. Seterusnya, kertas kerja ini mencadangkan satu algoritma untuk pemeriksaan visual PCB secara automatik yang berupaya mengesan dan menyari kecacatan pada PCB. Algoritma ini dijalankan pada resolusi kasar pembezaan imej bertujuan untuk mengesan kawasan kecacatan pada resolusi halus imej PCB yang di periksa.

*Kata kunci:* pengesanan kecacatan, resolusi kasar, wavelets, pemeriksaan PCB

### 1.0 INTRODUCTION

There exist numerous algorithms, technique and approaches in the area of automated visual PCB inspection nowadays. As proposed by Moganti [1-2], these can be divided

<sup>1</sup> Department of Mechatronics and Robotics Engineering, Faculty of Electrical Engineering, Universiti Teknologi Malaysia, 81310 Skudai, Johor Darul Takzim, Malaysia. Email: zuwairie@fke.utm.my  
<sup>2&3</sup> Department of Microelectronics and Computer Engineering, Faculty of Electrical Engineering, Universiti Teknologi Malaysia, 81310 Skudai, Johor Darul Takzim, Malaysia. Email: syed@fke.utm.my<sup>2</sup>, zulfakar@fke.utm.my<sup>3</sup>

into three main approaches: referential approaches, rule-based approaches and hybrid approaches.

For the referential approaches, there are two major techniques. The first one is image comparison technique and the other one is model-based technique. The major shortcoming if this approach is related to image alignment or registration for comparison purpose.

The simplest operation of image comparison technique is realized by comparing the tested PCB image against the reference PCB image using simple XOR logic operator. Instead of XOR logic operator, image mathematical operation is also useful. For instance, the work carried out by Wen-Yen, et al. [3] did the direct subtraction of the reference to the test image to produce *Positive (P)*, *Negative (N)* and *Equal (E)* pixels. After that, the defect detection and classification are done based on the *P*, *N* and *E* pixels.

Model-based technique on the other hand, matches the tested PCB image with a predefined model. An early proposal use graph-matching technique. Under this technique, the defective PCB image can be successfully recognized but the position of each defect cannot be located. The major difficulty of this method is related to the matching complexity. Ja and Yoo [4] introduced tree representation scheme for PCB inspection. Although the tree representation technique is less complex than the graph-matching technique, yet the location of the defects still cannot be retrieved. Another method compares two PCB images based on their connectivity [5] but the connectivity defects are limited to short circuit and open circuit only.

The inspiration to process the PCB images in run length encode (RLE) is realized by Ercal, et al. [6] and Hou, et al. [7]. Under this idea, the binary PCB image is converted to RLE data. Consequently, they come out with a systolic algorithm to produced differenced image but the process is applied on RLE data.

Rule-based approaches test the design rule of the PCB traces to determine whether each PCB trace fall within the required dimensions or not. Mathematical morphological operation is frequently used where dilation and erosion are the basic operation [8-11]. The main advantage of the design-rule checking approach is it does not require a reference PCB image. Thus, this approach is not subjected to the alignment problem. Since they verify the design-rule, the disadvantage is they might miss defects that do not violate the rules. Furthermore, rule standardization is needed for the entire image of the inspected PCBs.

Lastly, the hybrid approaches combines the referential approaches and the design-rule approaches to make use the advantages and to overcome the shortcoming of each approach. But it is a complex and very time consuming process because it involved some sort of double-checking procedure.

This paper is organized as follows. Section 2 highlights the research methodology of this project. The proposed algorithm consist of 2 stages: the defect detection and the defect localization. The wavelet-based image difference algorithm is described

briefly in section 3. The coarse resolution defect localization algorithm is addressed clearly in section 4. The proposed defect localization algorithm entirely can be divided into four operations: connected-component labeling operation, window coordinates searching operation, mapping operation and windowing and defect extraction operation. Section 5 contains the conclusions of this paper. Lastly, the references of this research work are placed in section 6.

## 2.0 RESEARCH METHODOLOGY

Numerous techniques, methods and algorithms have been proposed for the automated visual PCB inspection. The latest technique is cited in [12-13]. All these techniques, methods and algorithms concentrate mainly on the defect detection. Obviously, none of them mentions the defect localization and extraction which are the subsequent stage after the defect detection is completely done. Defect localization and extraction are important in order to provide the information to the operator where exactly each defect occurred. It is also important for the purpose of defect classification.

This paper tackles the problem of the automated visual PCB inspection from a different point of view. For the defect detection, the wavelet-based image difference algorithm as proposed in [13] is selected. Then, the defect localization stage will be executed. The defect localization algorithm is computed on the coarse resolution differenced image, which is the output of the wavelet-based image difference algorithm. Lastly, the defective areas are windowed on the fine resolution original image of the tested PCB. This algorithm is also able to extract each defective area to provide adequate information for the subsequent stage after defect localization and extraction.

## 3.0 DEFECT DETECTION ALGORITHM

The wavelet-based image difference algorithm is selected for the defect detection algorithm. The algorithm provides an effective way to minimize the computation time of image difference operation for PCB defect detection algorithm. Firstly, this technique applies the second level Haar wavelet transform to both the reference and test PCB image. The reference PCB image and the test PCB image are shown in Figure 1 and Figure 2 respectively. Then, the image difference operation is computed by comparing the test PCB image against the reference PCB image in wavelet domain. Figure 3 shows the coarse resolution differenced image that is the output of the wavelet-based image difference algorithm. The flow of the algorithm is depicted in Figure 4.

..

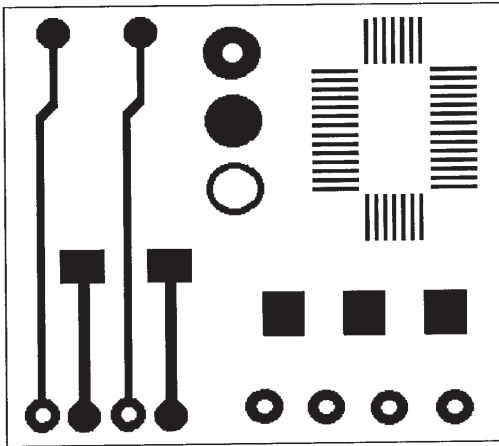


**Figure 1** A reference PCB image

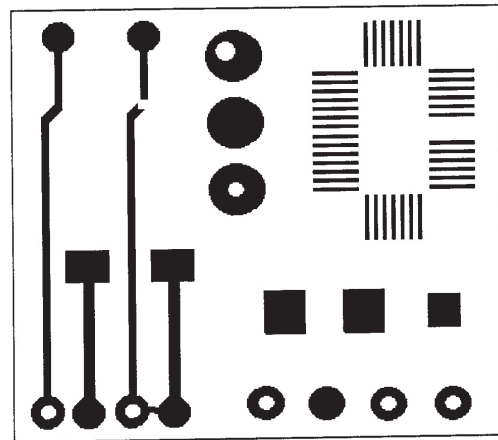


**Figure 2** A test PCB image

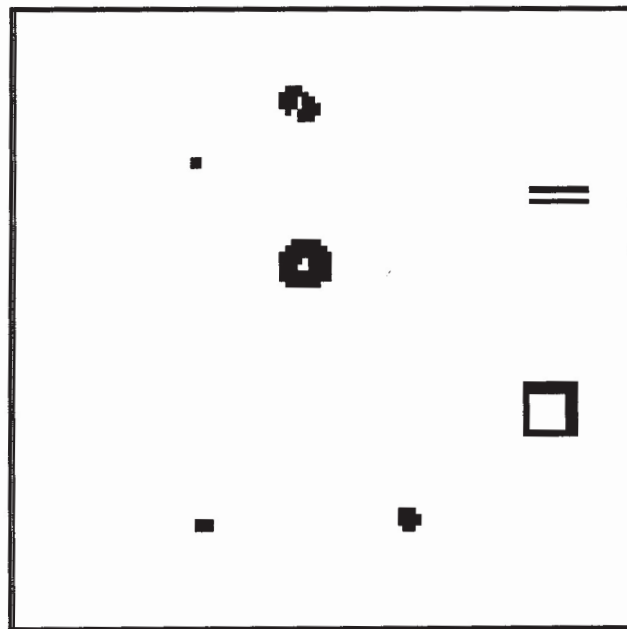


**Figure 3** Coarse resolution differenced image

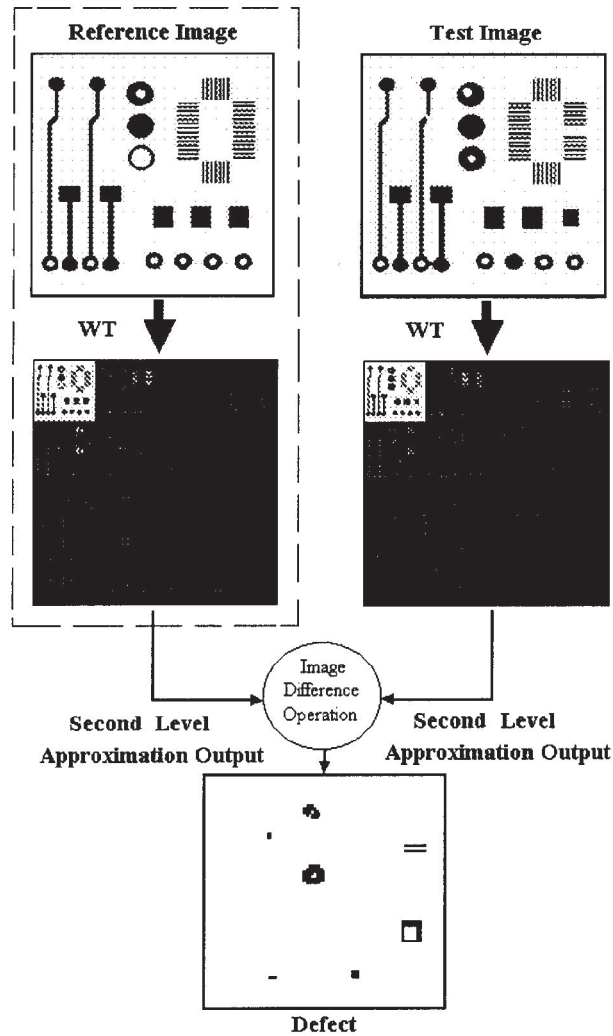


**Figure 4** Wavelet-based image difference algorithm

#### 4.0 DEFECT LOCALIZATION ALGORITHM

The purpose of the defect localization algorithm is to highlight the defective areas on the tested PCB image. Defect localization is important in order to inform operators about the location of the defects detected for further procedures such as defect classification and defect marking.

The input for the defect localization algorithm is the coarse differenced image. The defect localization algorithm consists of four core operations, namely: connected-component labeling operation, window coordinates searching operation, mapping operation and windowing and defect extraction operation.

#### 4.1 CONNECTED-COMPONENT LABELING OPERATION

Before the connected-component labeling operation is explained, it is essential to understand the meaning of connectivity in a two-dimensional array or image. For a two-dimensional array, there exist two types of connectivity. The first one is 4-connected pixel and the second one is 8-connected pixel [14].

The 4-connected pixels are connected if their edges touch. This means that a pair of adjoining pixels is part of the same object only if they are both on and are connected along the horizontal or vertical direction. The 8-connected pixels are connected if their edges or corners touch. This means that if two adjoining pixels are on, they are part of the same object, whether they are connected along the horizontal, vertical, or diagonal direction. Figure 5(a) and Figure 5(b) represent the concept of a 4-connectivity pixel and an 8-connectivity pixel respectively.

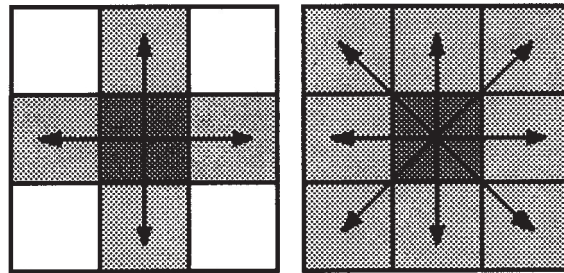


**Figure 5** (a) A 4-connectivity pixel (b) An 8-connectivity pixel

The connected-component labeling operation returns the information of the coarse differenced image (a binary image) to identify each object in the image. The output of the connected-component labeling operation is a two-dimensional output array named as labeled image. The size of the labeled image is exactly the same as the coarse differenced image, which the objects in the coarse differenced image are distinguished by different integer values in the labeled image. As an example, consider a small area of a coarse differenced image represented in two-dimensional  $10 \times 10$  array as shown in Figure 6.

The output array of the 4 connected-component labeling is depicted in Figure 7. This figure obviously shows that the connected-component labeling operation successfully recognizes 3 objects in the coarse differenced image. In this case, each object is assigned with an identical value starting from 1 to 3. This identical value depends on the number of objects in the coarse differenced image.

Figure 8 shows the output array of the 8 connected-component labeling operation. Compared to the output in Figure 7, the objects identified as 1 and 2 are merged to become one individual object because of the 8-connectivity factor chosen for the

0	0	0	0	0	0	0	0	0	0
0	0	0	0	0	0	1	1	1	0
0	0	0	0	0	0	1	1	1	0
0	0	0	0	0	0	0	1	0	0
0	1	1	1	0	0	0	0	0	0
0	1	1	1	0	0	0	0	0	0
0	1	1	1	0	0	0	0	0	0
0	1	1	1	0	0	0	0	0	0
0	0	0	0	1	1	1	0	0	0
0	0	0	0	1	1	1	0	0	0
0	0	0	0	1	1	1	0	0	0

**Figure 6** An example of a small area in a coarse differenced image

0	0	0	0	0	0	0	0	0	0
0	0	0	0	0	0	3	3	3	0
0	0	0	0	0	0	3	3	3	0
0	0	0	0	0	0	0	3	0	0
0	1	1	1	0	0	0	0	0	0
0	1	1	1	0	0	0	0	0	0
0	1	1	1	0	0	0	0	0	0
0	1	1	1	0	0	0	0	0	0
0	0	0	0	2	2	2	0	0	0
0	0	0	0	2	2	2	0	0	0
0	0	0	0	2	2	2	0	0	0

**Figure 7** The output of the 4 connected-component labeling operation

0	0	0	0	0	0	0	0	0	0
0	0	0	0	0	0	2	2	2	0
0	0	0	0	0	0	2	2	2	0
0	0	0	0	0	0	0	2	0	0
0	1	1	1	0	0	0	0	0	0
0	1	1	1	0	0	0	0	0	0
0	1	1	1	0	0	0	0	0	0
0	1	1	1	0	0	0	0	0	0
0	0	0	0	1	1	1	0	0	0
0	0	0	0	1	1	1	0	0	0
0	0	0	0	1	1	1	0	0	0

**Figure 8** The output of the 8 connected-component labeling operation

connected-component labeling operation. Thus, the total number of objects identified in the coarse differenced image is only 2.

In this project, the 8-connectivity pixel for the connected-component labeling operation is selected. This is to minimize the number of the identified object. In fact, each object representing a defective area and normally, defects are far apart from each other. As a result, the computation time of the overall wavelet-based PCB defect detection and localization algorithm can be minimized. This operation is done on the coarse resolution image.

#### 4.2 WINDOW COORDINATES SEARCHING OPERATION

The resultant image of 8 connected-labeling operation is taken to be an input for the window coordinate searching operation. Here, the result in Figure 8 is taken as an input for the ease of explanation. The most important objective of this operation is to search for four coordinates of each object in Figure 8 for the defective area windowing. The four coordinates of each object are named as: *RowMin*, *RowMax*, *ColMin* and *ColMax* which correspond to minimum row, maximum row, minimum column and maximum column respectively. Note that this operation is done on the coarse resolution image. With Figure 8 as the input image for window coordinate searching operation, the output of this operation is shown in Table 1. As an example, Figure 9 represents the location of the *RowMin*, *RowMax*, *ColMin* and *ColMax* for the object identified by number 2 in a  $10 \times 10$  array.

**Table 1** Output of window coordinate searching operation

Object	RowMin	RowMax	ColMin	ColMax
1	5	10	2	7
2	2	4	7	9

#### 4.3 MAPPING OPERATION

According to the coordinates obtained in window coordinate searching operation, a number of windows are drawn on the fine resolution tested image. Recall that these four coordinates of each object is defined in a coarse resolution image. Hence, some sort of mapping equation is needed to map the coordinates in the coarse resolution image to the fine resolution image. The determination of the mapping equation is critical in the sense that ineffective mapping equation will cause the distortion problem happened to the individual drawn window. In order to derive the mapping equation employed in this paper, four coordinates *RowMin*, *RowMax*, *ColMin* and *ColMax* represented in Figure 9 is selected again. These four coordinates are chosen to simplify the justification of the mapping equation.



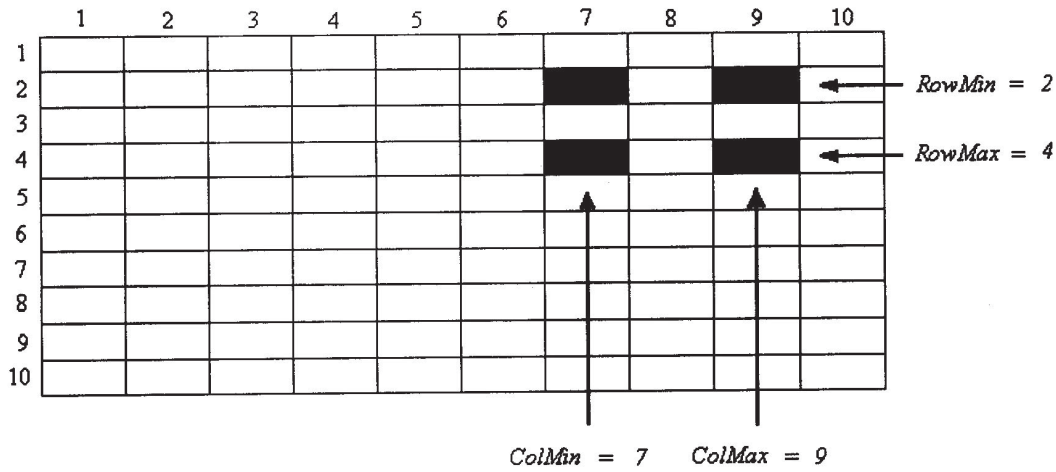


**Figure 9** Representation of *RowMin*, *RowMax*, *ColMin* and *ColMax* for the object number 2

If the  $10 \times 10$  array in Figure 9 is to be enlarged into a  $80 \times 80$  array, as an example, the output of the image enlargement should be as depicted in Figure 10. In this case, the enlargement coefficient, *E* is 8. Apparently, each four point as small as one pixel is enlarged to be  $8 \times 8$  pixels in the enlarged image. Then, each coordinate is mapped into 8 possible values actually as shown in Figure 10. However, for the windowing operation, the mapping equation should be able to accomplish one point to one point mapping. In order to solve this matter, two simple sets of rules are considered.

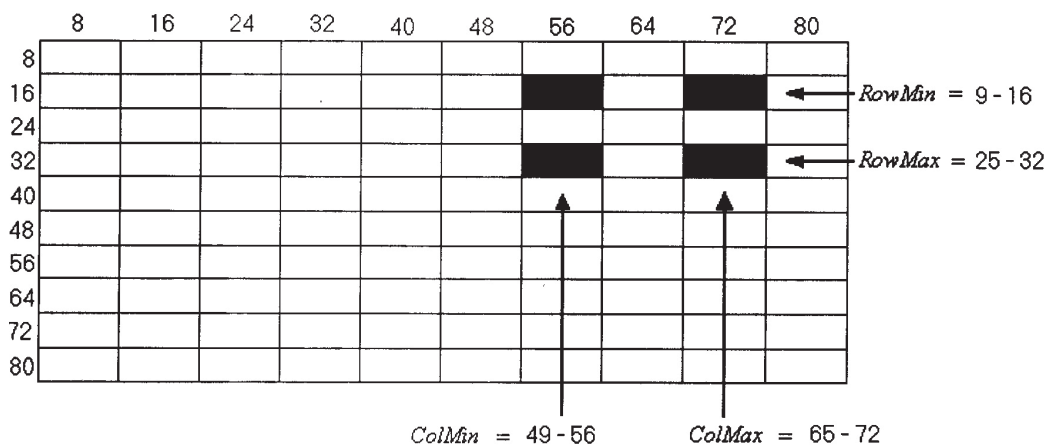


**Figure 10** The resized image (enlargement coefficient, *E* = 8)

Suppose that if each coordinate  $RowMin$ ,  $RowMax$ ,  $ColMin$  and  $ColMax$  on the coarse resolution image is mapped into  $RowL$ ,  $RowH$ ,  $ColL$  and  $ColH$  on the fine resolution image:

1. The value of  $RowL$  and  $ColL$  should be the minimum value within the range of possible values.
2. The value of  $RowH$  and  $ColH$  should be the maximum value within the range of possible values.

Based on the rules, the equation 1, 2, 3 and 4 are effectively can be used for the mapping operation.

$$RowL = (RowMin)(E) - (E - 1) \quad (1)$$

$$RowL = (RowMin)(2^L) - (2^L - 1)$$

$$RowH = (RowMax)(E) \quad (2)$$

$$RowH = (RowMax)(2^L)$$

$$ColL = (ColMin)(E) - (E - 1) \quad (3)$$

$$ColL = (ColMin)(2^L) - (2^L - 1)$$

$$ColH = (ColMax)(2^L) \quad (4)$$

$$ColH = (ColMax)(2^L)$$

where  $E = 2^L$  and  $L$  denotes the iteration or level of wavelet transform used in the wavelet-based image difference algorithm. In this project,  $L = 2$  is chosen in order to obtain an effective inspection time without increasing the computation cost of the inspection system [15].

#### 4.4 WINDOWING AND DEFECT EXTRACTION OPERATION

For each  $RowL$ ,  $RowH$ ,  $ColL$  and  $ColH$  related to each defective area, a boundary line representing a window can be drawn on the fine resolution tested PCB image. Each window marks the defective areas where the defects are actually occurred. After the defective areas are windowed successfully, it is possible to segment each defective area for defect extraction where each defective area is shown in an individual image.

The result of the defect localization is depicted in Figure 11. The black windows on the gray pattern highlight the defective areas on the tested PCB image. The flow of the proposed algorithm is shown in Figure 12. Lastly, the overall flow of the PCB defect detection and localization algorithm is depicted in Figure 13.

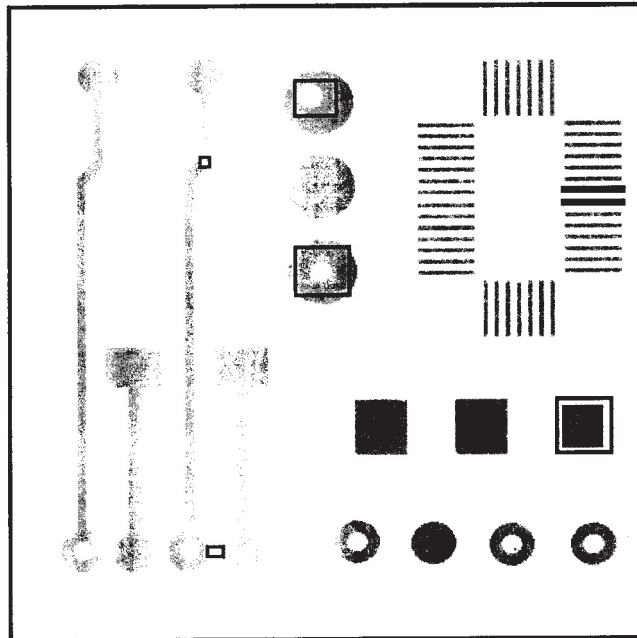


**Figure 11** Defect localization

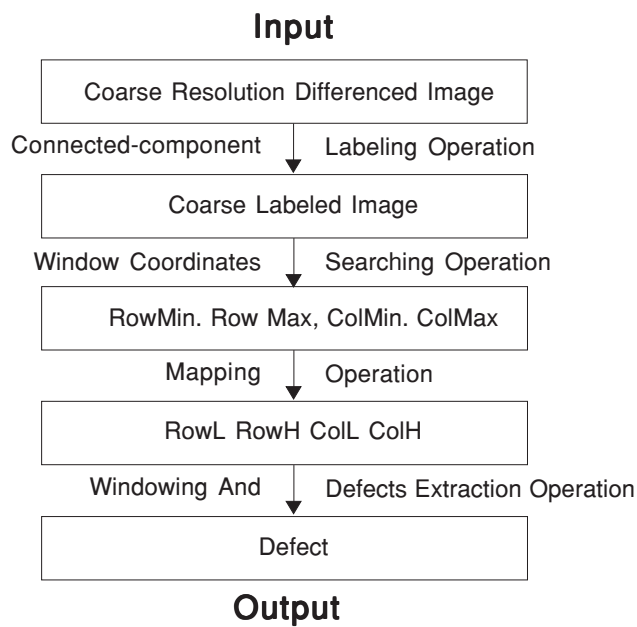


**Figure 12** Coarse resolution defect localization algorithm

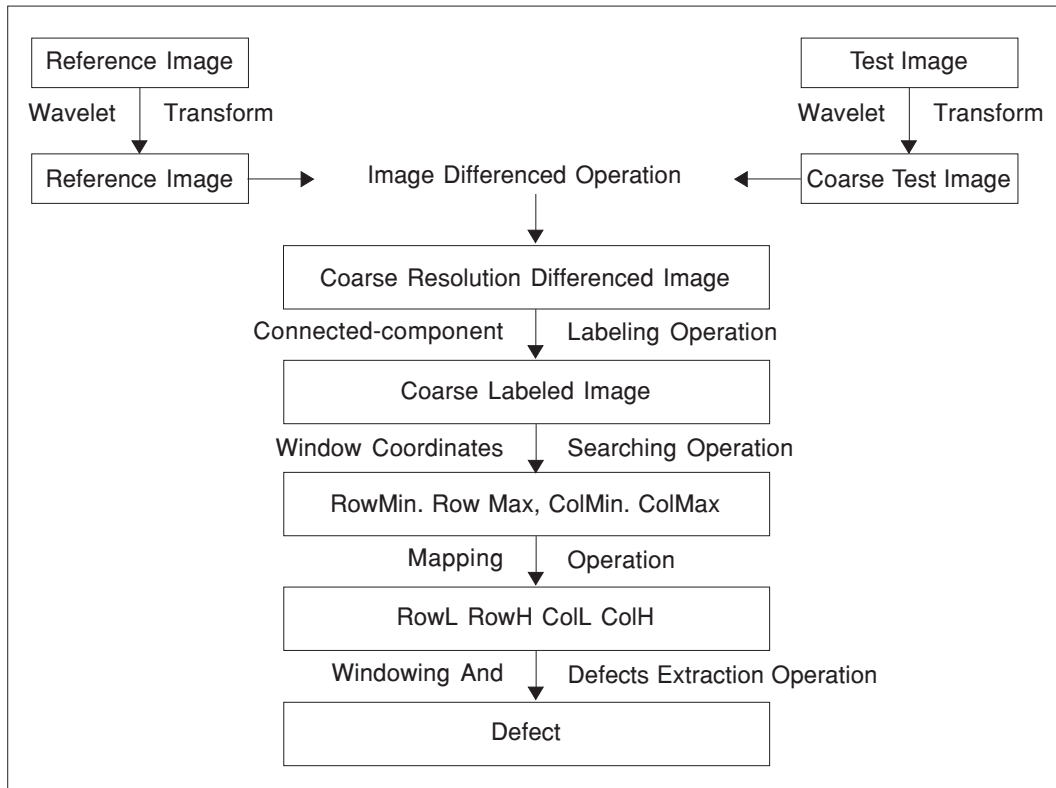


**Figure 13** Overall flow of the PCB defect detection and localization algorithm

## 5.0 CONCLUSIONS

This paper proposes an algorithm for PCB defect localization for an automated visual PCB inspection. The localized area in the tested PCB image will be used as the inputs to the classification stage, which is the subsequent stage after the defect detection has been done. The continuation of this research is to implement the algorithm on hardware to ensure that the automated visual PCB inspection system can perform in a real-time environment with high efficiency.

## REFERENCES

- [1] Moganti, M., F. Ercal, C. H. Dagli, and S. Tsunekawa. 1996. Automatic PCB Inspection Algorithms: A Survey. *Computer Vision and Image Understanding*. 63(2): 287-313.
- [2] Moganti, M., and F. Ercal. 1995. Automatic PCB Inspection Systems. *IEEE Potentials*. 14(3): 6-10.
- [3] Wen-Yen, W., J. W. Mao-Jiun, and L. Chih-Ming. 1996. Automated Inspection of Printed Circuit Boards Through Machine Vision. *Computers in Industry*. 28(2): 103-111.
- [4] Ja, H. K., and S. I. Yoo. 1998. A Structural Matching for Two-dimensional Visual Pattern Inspection. *IEEE International Conference on Systems, Man and Cybernetics*. 5. 4429-4434.

- [5] Tatibana, M. H., and R. A. Lotufo. 1997. Novel Automatic PCB Inspection Technique based on Connectivity. *Proceedings of Brazilian Symposium on Computer Vision and Image Processing*. 187-194.
- [6] Ercal, F., F. Bunyak, H. Feng, and L. Zheng. 1997. A Fast Modular RLE-based Inspection Scheme for PCBs. *Proceedings of SPIE – Architectures, Networks and Intelligent Systems for Manufacturing Integration*. 3203. 45-59.
- [7] Hou, F., F. Ercal, and F. Bunyak. 1998. Systolic Algorithm for Processing RLE Images. *Proceedings of IEEE Southwest Symposium on Image Processing and Interpretation*.
- [8] Oguz, S. H., and L. Onural. 1991. An Automated System for Design-Rule-Based Visual Inspection of Printed Circuit Boards. *Proceedings of the IEEE International Conference on Robotics and Automation*. 2696-2701.
- [9] Darwish, A. M., and A. K. Jain. 1988. A Rule Based Approach for Visual Pattern Inspection. *IEEE Transaction of Pattern Analysis and Machine Intelligence*. 10(1): 56-58.
- [10] Qin-Zhong, Y., and P. E. Danielson. 1998. Inspection of Printed Circuit Boards by Connectivity Preserving Shrinking. *IEEE Transaction on Pattern Analysis and Machine Intelligence*. 10(5): 737-742.
- [11] Mesbahi, J. E., and M. Chaibi. 1993. Printed Circuit Boards Inspection Using Two New Algorithms of Dilation and Connectivity Preserving Shrinking. *Proceedings of the 1993 IEEE-SP Workshop on Neural Networks for Processing*. 527-536.
- [12] Zuwairie, I., S. A. R. Al-Attas, Z. Aspar, and R. Ghazali. 2001. Performance Evaluation of Wavelet-Based Algorithm for Printed Circuit Board (PCB) Inspection. *Jurnal Teknologi*. 35(D): 39-54.
- [13] Zuwairie, I. 2002. *Printed Circuit Board Inspection Using Wavelet-based Technique*. M. Eng. Thesis: Universiti Teknologi Malaysia, Malaysia.
- [14] Masiti, M., Y. Masiti, G. Oppenheim, and J. Poggi. 1997. *Wavelet Toolbox: For Use with MATLAB*. USA: The Math Works Inc. 1-1-1-36.
- [15] Zuwairie, I., S. A. R. Al-Attas and Z. Aspar. 2002. Analysis of the Wavelet-based Image Difference Algorithm for PCB Inspection. *Proceedings of the 2002 41st SICE Annual Conference (SICE 2002)*: 1525-1530.